What if you eat nanoplastics? Simulating nanoplastics fate during gastrointestinal digestion

Supplementary Information

Table S1. Previous research on macro-, micro- and nanoplastic fate during *in vitro* gastrointestinal digestion

Polymer and particle size; concentration	**Analytical techniques used**	**Findings**	**Ref.**
PSL 3.8 μm, other conventional polymers >60 μm; 10-100 mg/mL intestinal juice	Scanning electron microscopy (SEM)	Massive protein corona formation, especially on the smaller particles No change in sizes of larger particles Measured increase in size of the smallest PS particles, shown to be due to interactions with proteins in the digestive juices	(Stock et al., 2020)
PSL25, PSL1000, PSL25-f, PSL100-f, PSL1000-f PE<2.5 μm; 0.1-0.25 mg/mL intestinal juice	Multi-angle light diffraction (MALD), confocal microscopy, used cell line Caco-2	After digestion all particles formed two size populations: 3–5 μm and >10 μm After digestion PSL formed wider size distributions, agglomerates PSL-f agglomerated to a smaller degree than PSL Some 1000 nm particles remained in the original size PE size distribution shifted towards smaller sizes	(DeLoid et al., 2021)

		Probably non-endocytic mechanism of entry (e.g. diffusion across the membrane) NPLs increased permeability of the cells (especially PSL-f) PSL25-f agglomerates were found inside cell nuclei Greater translocation of PSL25-f than for PSL1000-f	
PLGA 10 μm, PE 10 μm, PVC 1 μm, PET 50 μm PS 50 nm, 1 μm, 10 μm; 0.08 mg/mL intestinal juice	Laser scanning confocal microscopy; ATR-FTIR (for investigation of PSL-enzyme adsorption)	All tested particles reduced lipid digestion, PVC and PLGA to a smaller extent Particle size did not significantly influence lipid digestion but particle concentration did Free fatty acids formed agglomerates with particles Multiple lipid droplets formed agglomerates with single PSL PSL were negatively charged down to pH 2.5 Presence of PSL did not affect pepsin activity	(Tan et al., 2020)
Bulk 0.5 cm pieces of PS and HDPE from food packaging	microscopy FTIR	MNPs were released from the plastic pieces after digestion (from both plastic types but from HDPE to a higher extent) Surface of HDPE became rough and cracked after digestion	(Krasucka et al., 2022)

		Oxidation of the HDPE surface after digestion Degradation of the C=O groups previously present on the surface of the PS product Decrease of hydrophobicity on the surface of both plastics	
PLA 2 µm, PLA 250 nm, melamine formaladehyde resin particles 366 nm, PMMA 25 nm, concentrations given as particle surface are per milliliter	DLS, AF4-MALS, SEM Cell viability assays on the Caco-2 cell culture	Particles difficult to detect by SEM because of the dried organic fluids No effect of saliva on the PLA250 size but size increase after gastric stage Smaller PLA particles agglomerated to the higher extent than the larger ones PLA particles agglomerated more than PMMA and melamine formaldehyde resin	(Paul et al., 2024)

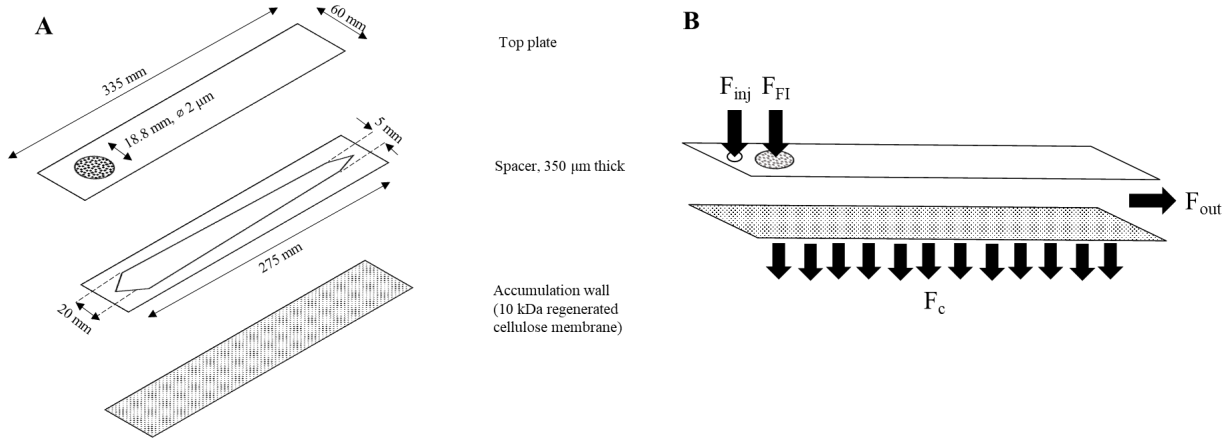

Figure S1. A) AF4 separation block. B) In- and outflows of the AF4 separation block.

Table S2. FI-AF4 method flow program.

Injection	Injection flow (F_{inj})	0.05 mL/min
	Crossflow (F_c)	2 mL/min
	Frit-inlet flow (F_{FI})	2.45 mL/min
	Detector flow (F_{out})	0.50 mL/min
Elution	Crossflow (F_c)	Constant at 2 mL/min for 2 mins Exponential decay (exp=0.05) down to 0 mL/min over 30 mins Constant at 0 mL/min for 10 mins
	Detector flow (F_{out})	0.50 mL/min

Section S1. Choice of FI-AF4 carrier liquid

Nanoparticles are commonly analyzed with AF4 using carrier liquids of very low ionic strength or surfactants to prevent their agglomeration. Proteins, on the other hand, generally require high ionic strength to hamper them from interacting with the membrane.(Condado-Morales et al., 2023) Sodium dodecyl sulphate (SDS) is a surfactant, and its applicability has been shown in the separation of pepsin and metallic nanoparticles by Böhmert et al. (Böhmert et al., 2014), therefore, the same carrier liquid was also used in this study.

$$P(\vartheta) = \left(\frac{3}{h^3}(sinh - hcosh)\right)^2$$

Eq. S1. Form factor applied in calculation of radii of gyration in the Sphere model

Where:

$P(\vartheta)$-form factor of the sample

ϑ-scattering angle

$h = r_G \frac{4\pi n}{\lambda} \sin\frac{\vartheta}{2}$

n – refractive index of the carrier liquid

λ - wavelength of the incident light

r_G– size

$$\sqrt{\frac{Kc}{R(\vartheta)}} = \sqrt{\frac{1}{M}\{1 + \frac{2}{3!}\left[\frac{4\pi}{\lambda} r_G \sin\left(\frac{\vartheta}{2}\right)\right]^2\}}$$

$$R(\vartheta) - Rayleigh\, ratio$$

Eq. S2. Equation describing the Berry model

Table S3. Results of DLS measurements performed immediately (no incubation).

Experiment	**Particles**	**r_H in ultrapure water**	**r_H after gastric stage [nm]**	**r_H after gastrointestinal stage [nm]**

		[nm]		
pH	PSL50	30.1±0.7	28.3±0.9	30.5±0.9
	PSL50-f	29.9±0.8	29.6±3.3	27.5±2.0[a]
	PSL200	119.6±3.1[a]	103.4±2.2	116.7±4.6[a]
	PLGA	34.6±9.4	129.1±24.8	144.3±12.4[a]
	PLGA+PSL50	39.3±9.1	149.5±16.6	141.7±16.7
			25.4± 7.9 (n=14/21)[b]	25.7±7.5 (n=12/20)[b]
pH+NaCl	PSL50	Not measured	41.0±2.1	96.5±21.5[a]
	PSL50-f		29.5±5.2	28.3±2.6
			194.9±58.8 (n=13/20)[b]	
	PSL200		123.6±7.0	127.9±6.9[a]
	PLGA		145.8±8.4	169.2±21.0[a]
	PLGA+PSL50		179.4±12.3[a]	238.8±34.8[a]

[a]a small signal around 2-11 nm

[b]signal detected in n replicates out of the total number of measurements

Section S2. FI-AF4-UV-MALS and in vitro gastrointestinal digestion method development for polystyrene nanoparticles

Initial experiments carried out on a simple PSL50-pepsin-HCl pH 3 mixture (not incubated at physiological temperature) revealed the propensity of the enzyme to physically interact with the particles. As shown in Fig. S2, a mixture measured immediately yields two well-separated peaks. Since in AF4 the elution order is from the analytes of smallest sizes towards the larger ones, the first peak (around 5 mins) was assigned to pepsin and the second one (around 11 mins) corresponds to the PSL50 (blue trace). However, the measurement of the same mixture performed after 45 mins results in a visually different fractoram (red trace). The peak around 11 mins is much lower and slightly shifted towards higher t_r, indicating much fewer PSL50 in roughly intact state in the mixture and their slight increase in size. The r_G obtained by MALS also increased, from ~20-80 nm measured immediately to ~35-100 nm after 45mins. The enzymatic peak around 5 mins increased in size and a residual peak after 35 mins, when the separation force (crossflow) is reduced to 0, becomes well-visible. The same tendency is observed after 90 mins (yellow trace), with the r_G slightly increasing from ~40 to 110 nm. The increasing residual peak indicates formation of large agglomerates, with sizes exceeding the FI-AF4 separation capacity. The increasing enzymatic peak, in turn, is more difficult to explain. We hypothesize that some agglomerates are large enough to elute in the so-called steric mode, i.e., the size of the analyte is bigger than its mean movement from the AF4 accumulation wall caused by Brownian motion. Therefore, even without large diffusion towards the middle of the AF4 channel the analytes are still affected by the higher velocities of the laminar flow and they elute in the reversed elution order (steric elution) (see further explanation in (Giddings & Myers, 1978)). While accurate definition of the steric inversion point was out of the

scope of this research, according to a study on steric elution in FI-AF4 (Kim et al., 2018) in conditions roughly comparable to the ones applied herein, conglomerates larger than 1 µm could possibly elute in the steric mode. The important role of the digestive enzymes on the NPLs agglomeration suggested before has therefore been shown in this study.

To study the durability of the PSL50-pepsin agglomerates, five PSL50 gastric digesta were measured, each submitted to different vortexing times, ranging from 0 to 40 s. The resulting overlayed fractogram is shown in Fig. S3. As visible, vortexing results in appearance of a separate

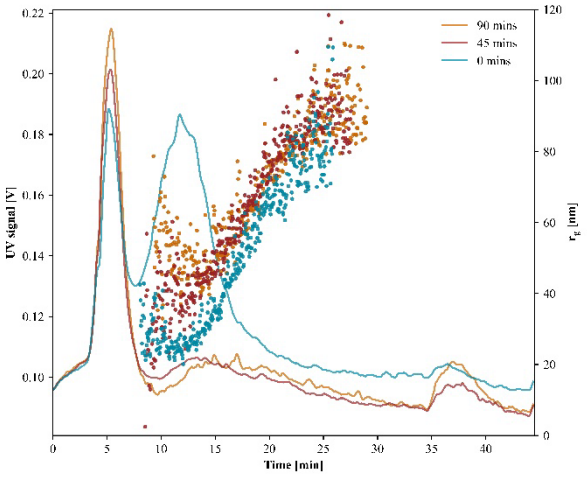

Figure S2. Influence of time on FI-AF4 separation ofpepsin-PSL50 mixture in pH 3. V_{inj}=2 µL

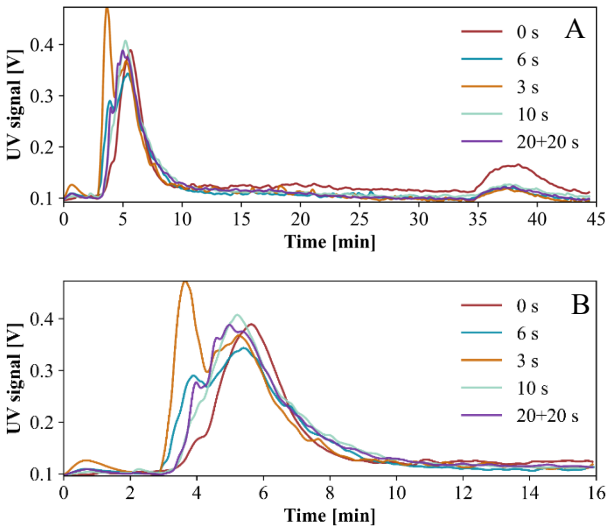

Figure S3. Influence of vortexing time on FI-AF4 separation of PSL50 gastric digest. A) Full fractogram B) The region of interest

peak with t_r<4 mins, whose intensity decreases with increase in vortexing time. The second peaks are also shifted towards shorter elution times. From those observation it can be concluded that the agglomerates resulting from the gastric digestion are delicate and can be redispersed. In further experiments, digesta samples were therefore measured after mild handshaking only. The fractograms also support the hypothesis about the steric elution.

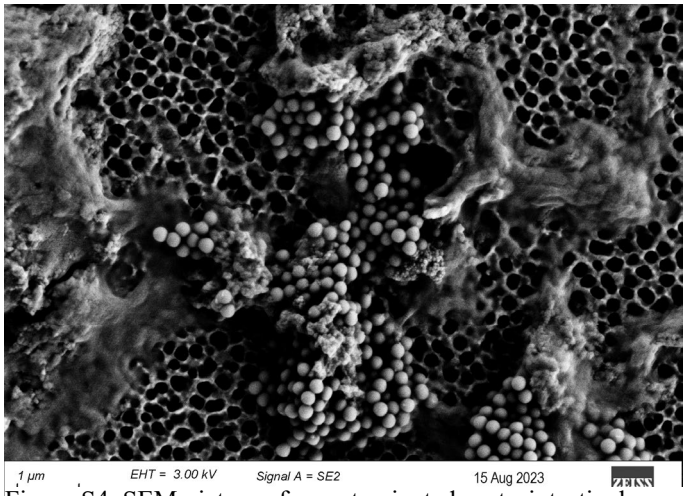

Figure S4. SEM picture of a contaminated gastrointestinal juice sample

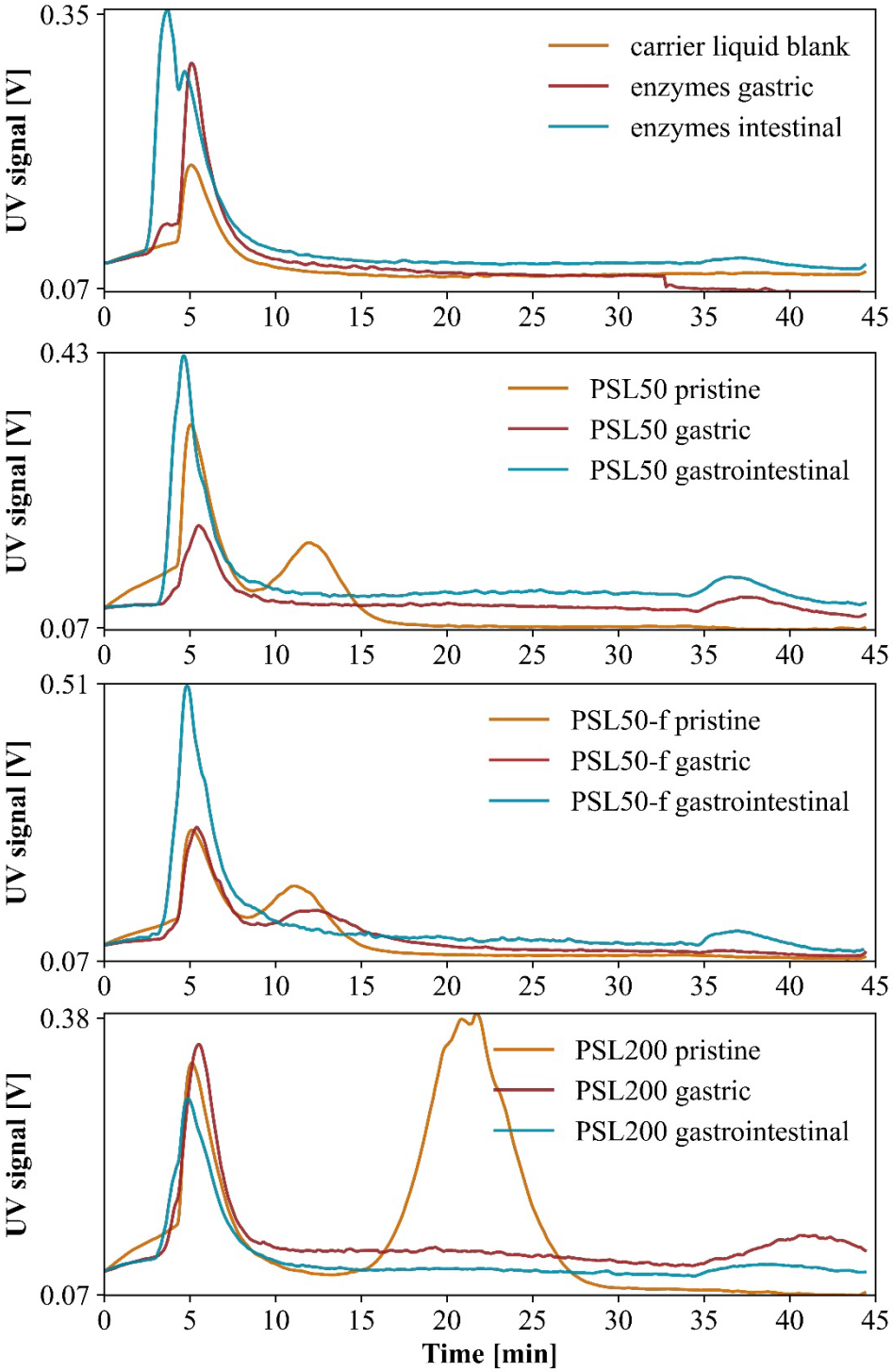

Figure S5. Fractograms resulting from the FI-AF4 analysis of the digesta.

Table S4. Limitations and justifications of use of the three analytical techniques applied in this study.

Technique	Limitation	Reasoning for applying the technique in this study
DLS	Accuracy of the results decreases with increasing size polydispersity; most suitable for narrow size distributions (Enfrin et al., 2021).	DLS was employed to estimate the average size (hydrodynamic radius) and polydispersity of nanoplastics. Because of the large difference between hydrodynamic radii of nanoparticles and enzymes, the digesta samples are considered too polydisperse for DLS. While we cannot use it to (accurately) study the digesta samples, which include enzymes, we used DLS to gain information on the influence of inorganic factors of the GIT (salinity, acidity, temperature, time of digestion) on the homoagglomeration of nanoplastics.
AF4-MALS	At high acidity and salinity (thus at conditions in the digesta samples) nanoparticles become more prone to interactions with each other and, probably, with the elements of the AF4 system. Using high flow rates that can be required for the fractionation of the samples, flows causing analyte separation in AF4 may exert high forces on the nanoparticles, impeding their elution within the elution window.	AF4-MALS was crucial for separating nanoparticles from enzymes and provided detailed size distributions, including the radius of gyration (r_G). This technique filled the gap left by DLS, allowing us to assess the influence of digestive enzymes on nanoplastic behaviour.
SEM	Provides primarily visual and qualitative information; challenging to measure the smallest particles.	SEM was utilized to visually confirm the findings from DLS and AF4-MALS, particularly under the most realistic digestive conditions (high acidity, high salinity, presence of enzymes). It provided essential morphological data to validate the trends observed with the other techniques.

References

Böhmert, L., Girod, M., Hansen, U., Maul, R., Knappe, P., Niemann, B., Weidner, S. M., Thünemann, A. F., & Lampen, A. (2014). Analytically monitored digestion of silver nanoparticles and their toxicity on human intestinal cells. *Nanotoxicology*, *8*(6). https://doi.org/10.3109/17435390.2013.815284

Condado-Morales, I., Sokolova, V., Wahlund, P.-O., Heding, K. E., Auclair, S., Kingsbury, J. S., Arosio, P., & Lorenzen, N. (2023). AF4 and PEG Precipitation as Predictive Assays for Antibody Self-Association. *Molecular Pharmaceutics*, *20*(2), 1323–1330. https://doi.org/10.1021/acs.molpharmaceut.2c00946

DeLoid, G. M., Cao, X., Bitounis, D., Singh, D., Llopis, P. M., Buckley, B., & Demokritou, P. (2021). Toxicity, uptake, and nuclear translocation of ingested micro-nanoplastics in an in vitro model of the small intestinal epithelium. *Food and Chemical Toxicology*, *158*, 112609. https://doi.org/10.1016/j.fct.2021.112609

Enfrin, M., Hachemi, C., Hodgson, P. D., Jegatheesan, V., Vrouwenvelder, J., Callahan, D. L., Lee, J., & Dumée, L. F. (2021). Nano/micro plastics – Challenges on quantification and remediation: A review. *Journal of Water Process Engineering*, *42*, 102128. https://doi.org/10.1016/j.jwpe.2021.102128

Giddings, J. C., & Myers, M. N. (1978). Steric Field-Flow Fractionation: A New Method For Separating I to 100 μm Particles. *Separation Science and Technology*, *13*(8). https://doi.org/10.1080/01496397808057119

Kim, Y. B., Yang, J. S., & Moon, M. H. (2018). Investigation of steric transition with field programming in frit inlet asymmetrical flow field-flow fractionation. *Journal of Chromatography A*, *1576*. https://doi.org/10.1016/j.chroma.2018.09.036

Krasucka, P., Bogusz, A., Baranowska-Wójcik, E., Czech, B., Szwajgier, D., Rek, M., Ok, Y. S., & Oleszczuk, P. (2022). Digestion of plastics using in vitro human gastrointestinal tract and their potential to adsorb emerging organic pollutants. *Science of The Total Environment*, *843*, 157108. https://doi.org/10.1016/j.scitotenv.2022.157108

Paul, M. B., Böhmert, L., Thünemann, A. F., Loeschner, K., Givelet, L., Fahrenson, C., Braeuning, A., & Sieg, H. (2024). Influence of artificial digestion on characteristics and intestinal cellular effects of micro-, submicro- and nanoplastics. *Food and Chemical Toxicology*, *184*, 114423. https://doi.org/10.1016/j.fct.2023.114423

Stock, V., Fahrenson, C., Thuenemann, A., Dönmez, M. H., Voss, L., Böhmert, L., Braeuning, A., Lampen, A., & Sieg, H. (2020). Impact of artificial digestion on the sizes and shapes of microplastic particles. *Food and Chemical Toxicology*, *135*. https://doi.org/10.1016/j.fct.2019.111010

Tan, H., Yue, T., Xu, Y., Zhao, J., & Xing, B. (2020). Microplastics Reduce Lipid Digestion in Simulated Human Gastrointestinal System. *Environmental Science & Technology*, *54*(19), 12285–12294. https://doi.org/10.1021/acs.est.0c02608